*e*JSE

International

Experimental & theoretical behavior of thin walled composite filled beams

Khandaker M. Anwar Hossain

BSc Eng, MSc Eng, PhD (Strath, UK) Department of Civil Engineering
University of Technology, Lae, Papua New Guinea
Currently working in Department of Civil Engineering
University of Toronto, Canada
E-mail: *dr_k_m_hossain@hotmail.com*

ABSTRACT

The behaviour of thin walled composite (TWC) filled beams with normal (NC) and lightweight volcanic pumice concrete (VPC) as in-fill, is described based on comprehensive series of tests. The strength and failure modes of the beams are found to depend on the interface connections. The effect of various modes interface connections are co-related to the generation of shear bond between sheeting and concrete using both experimental and theoretical results. Analytical models for the design of beams are developed and their performance is validated through experimental results using both full and partial connection. Appropriate design recommendations and practical design charts have been developed so that the designer can check whether the strength will be governed by buckling or yielding of steel and be able to design the beam accordingly.

KEYWORDS

Volcanic pumice, beam, thin walled, buckling, strength, lightweight, composite, flexural, analytical, interface, shear bond

1   Introduction

Thin walled composite (TWC) sections is a new idea for beams [1,2,3,4] comprising cold formed steel elements with an infill of concrete that are suitable as replacement for hot-rolled steel or reinforced concrete in small to medium sized building. Typical TWC beams are shown in Figure 1.
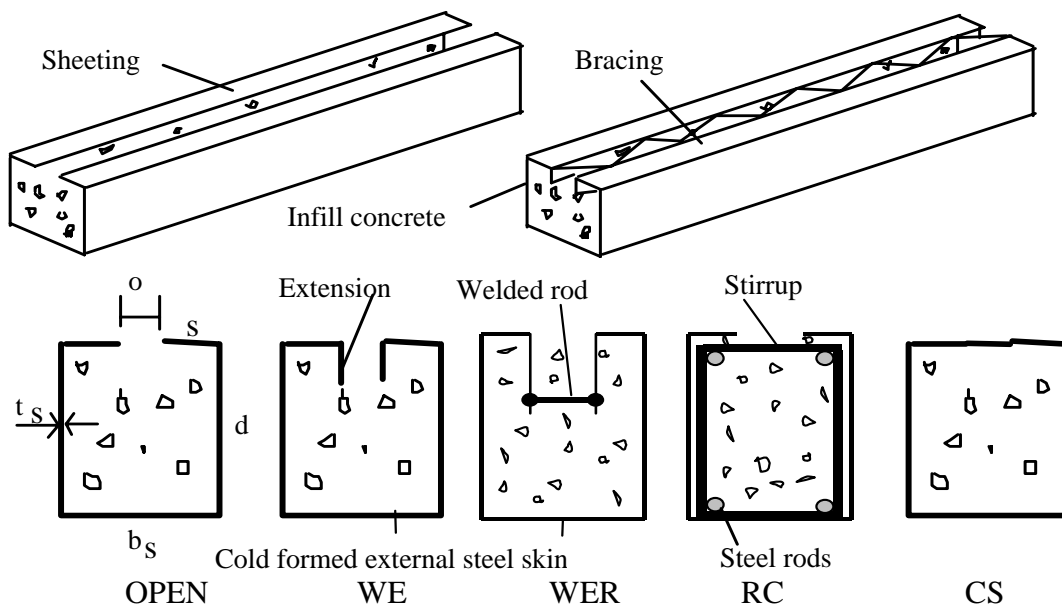

Figure 1: Geometric of composite beams

The inherent advantages of this system are derived from its structural configurations. Open box sections for beams will allow easy casting of in-fill concrete. TWC sections do not require temporary formwork for infill concrete as the steel acts as formwork in the construction stage and as reinforcement in the service stage. They are simple to fabricate and construct compared to conventional reinforced concrete where skilled workers are needed to cut and bent complex forms of reinforcement. The infill concrete is less likely to be affected by adverse temperature and winds as experienced in the case of reinforced concrete. The in-fill concrete is generally cured quickly and in any case, the load capacity of the steel alone may be relied upon for most construction loads. The steel sections can be designed, primarily, for the construction load of wet concrete, workmen and tools.

TWC sections are more susceptible to fire, although the thermal mass of the concrete infill provides reasonable protection to most fire loads. The smooth metallic finish of TWC sections is superior to conventional concrete and accepts more paint finish. Concrete filled steel elements as a means of providing aesthetic and economical structural elements attract interests in the construction industry.

Current study [5, 6] led to the development of novel form of thin walled composite (TWC) beams with recommendation on the use of VPC infill. One aspect of this research was to study the comparative performance of TWC beams with NC and VPC. Comprehensive research by Hossain [7, 8] on the properties of lightweight volcanic pumice concrete (VPC) suggested that, it is possible to obtain a VPC (1:2:4) of 30% lighter than normal concrete and having strength 30 MPa. The improved performance of VPC in a confined environment will allow the use of comparatively low strength VPC in this form of construction. Advantage of such TWC system includes a very light construction weight, excellent surface finish, relatively slender dimensions, enhanced ductility and the potential for semi-rigid connections.

This paper describes the performance of TWC beams with various interface connections and highlights the features to be included in the development of analytical models. The formulation of design guidelines for such beams especially using VPC will lead to the foundation of such construction using volcanic debris in the post-disaster rehabilitation projects of countries vulnerable to volcanic activities such as Papua New Guinea.

Table 1: TWC beam Details

Beam	Concrete		Steel	Dimensions, mm					Configuration
	Type	f'c MPa	f_{sy} MPa	b_s	d	o	y	t_s	
Series A : L=1500mm									
A1	NC	21	375	100	100	20	0	3.2	OS, NMR,NS
A2	NC	21	350	50	100	10	0	2.3	OS, NMR,NS
A3	VPC	20	375	100	100	20	0	3.2	OS, NMR, NS
A4	VPC	20	375	50	100	10	0	2.3	OS, NMR, NS
Series B: L = 600mm									
Filled									
B3Inc	NC	21	375	100	100	20	0	3.2	OS, NMR, NS
B3IInc	NC	21	375	100	100	100	0	3.2	CS, NMR, NS
B3IIvpc	VPC	20	375	100	100	100	0	3.2	CS, NMR, NS
B4IInc	NC	21	350	50	100	50	0	2.3	CS, NMR, NS
B4IIvpc	VPC	20	350	50	100	50	0	2.3	CS, NMR, NS
B3d/4nc	NC	21	375	100	100	20	25	3.2	WE,NMR, NS

| B3d/2nc	NC	21	375	100	100	20	50	3.2	WE, NMR, NS
B4Inc	NC	33.3	350	50	100	10	0	2.3	OS, NMR, NS
B4IIInc	NC	33.3	350	50	100	10	0	2.3	BS, NMR, NS
Unfilled									
B4III	None	--	350	50	100	10	0	2.3	BS
B4I	None	--	350	50	100	10	0	2.3	OS
Series C: L= 990 mm; fy=455MPa									
CB1	NC	21	257	150	250	35	0	1.6	WE, NMR,NS
CB2	NC	21	257	150	250	35	62.5	1.6	WE, NMR,NS
CB3	NC	21	257	150	250	35	62.5	1.6	WER,NMR, NS
CB4	NC	21	257	150	250	35	62.5	1.6	WE, NMR,NS
CB5	NC	33	275	150	250	35	125	1.6	WE,NMR,NS
CB6	NC	33	275	150	250	35	125	1.6	WER,NMR,NS
CB7	NC	33	275	150	250	35	0	1.6	OS,MR,NS
CB8	NC	33	275	150	250	35	0	1.6	OS,MR,S

2   Experimental Study

Comprehensive series of tests were conducted to study the behaviour of TWC beams. The test specimens were fabricated with varying geometric, material and interface connection parameters. Based on geometric and mode of connections, the beams were classified (detailed shown in (Figure 1) into open (OS), welded extension (WE), welded extension with rod (WER), braced (BS), closed (CS) and (e) RC filled. The experiments had been conducted in three series: Series A, B and C.

2.1   Description of Composite beams

A total of 4 beams designated as A1, A2, A3 and A4 were tested to study the performance of comparatively slender OS beams (Figure 1) with normal (NC) and lightweight pumice concrete (VPC) as in-fill. The details of the beams are presented in Table 1.

A total of 11 beams in series B consisting of three OS, four CS, two BS, two WE were tested to study the effect of connections enhancing the sheet-concrete interaction and effect of in-fill VPC. Two unfilled BS and OS steel skins were also tested to study the   performance compared with filled beams.   The details of such beams are presented Table 1. The welded extensions had full-length weld and the depth of welded extensions (y) used, were quarter (d/4) and half (d/2) of the depth of the beam.

A total of 8 beams, designated as CB, consisting of WE, WER and RC as shown in Figure 1 were tested. Detail of these beams is presented in Table 1. WE beams as shown in Figure 1 and 2 had 0.48mm welded extension plates tag welded at 150mm c/c while WER beams had provided with additional restraint to enhance the interaction between sheeting and concrete with 6mm rods welded to the bottom of the extension plate at 150mm c/c. WE and WER beams had welded extension up to about one quarter and half of the depth of the beam. To facilitate concrete casting, the extension plates were punched with 40mm diameter holes as shown in Figure 2.

WER Beams   RC filled beams (CB7-8)
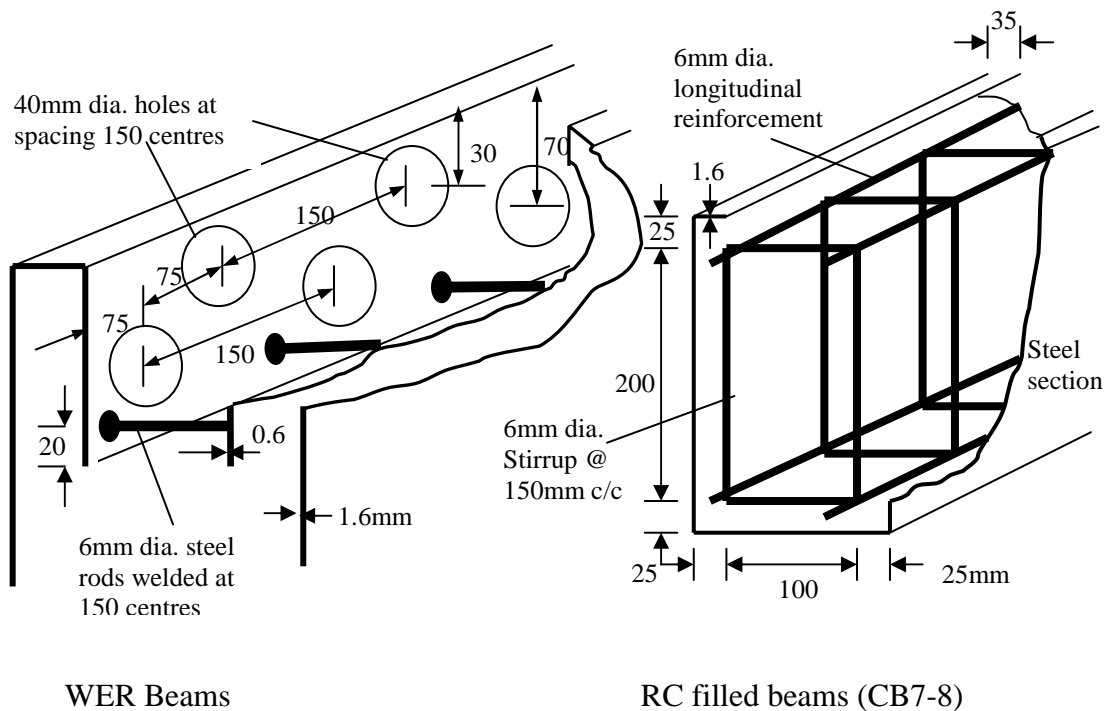
**Figure 2: Details of WE, WER and RC filled beams (C-series)**

RC beam CB7 was provided with only four 6mm rods as longitudinal reinforcements while CB8 had similar longitudinal reinforcements but with 6mm, U stirrups at 150mm center to center (Figure 2).

2.2   Casting and Curing of TWC beams

TWC specimens were cast in the Concrete Laboratory of Civil Engineering Department of Papua New Guinea University of Technology. The specimens were cast vertically with a natural sequence of their practical use in an especially fabricated stand. Care had been taken to avoid lateral buckling of thin steel plates especially for series C beams. Concrete was compacted in layers with portable poker vibrator. Control specimens in the form of cylinders and cubes were cast to determine the concrete strength. After 24 hours of casting, the control specimens and beams were demoulded and cured in open air until testing. The infill concrete for TWC beams either VPC or normal concrete (NC) was made from 20mm maximum size aggregates. Table 1 shows the steel and concrete properties of Series A, B and C beams. Cylinder ($f'c$) strength of concrete as well as yield strength of steel plate (f_{sy}) and rods (f_y) are presented.

2.3   Instrumentation and Testing

The strain gauges were installed at mid span of series A and C beams as shown in Figure 3 while no strain gauges were used in series B. The strain gauge 1 was installed at the centre of the bottom plate while gauges 2 and 3 were installed on the side steel plate 15mm from the top and bottom. Typical test setup for beam tested under two point loading condition is presented in Figure 3. The specimens were tested in a hydraulic testing machine. The load was applied at increments and at each load increment strains and central deformations are recorded to get complete load-deformation response. Central deflection was monitored by dial gauge. The strains were recorded by using manual electronic strain measuring equipment.
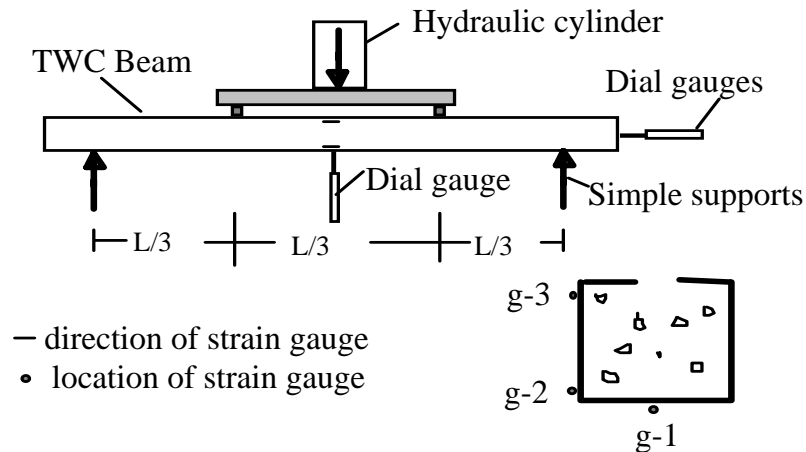
Figure 3: Test set-up and instrumentation of composite beams

Series A and C were tested under two point loading while the series B was tested under central single point loading condition. The overall behaviour of the beam including failure modes, cracking of concrete and buckling of steel plates was observed during the entire loading history.

## 2.4   Test observations and failure modes

The behaviour of the beams was affected by initial loss of chemical bond between the steel-concrete interfaces, presence of strength enhancement devices and flexural and shear reinforcement. During loading process (Figure 4), the beam underwent flexural deflection (stage 1), followed by separation (stage 2) of side steel plates from concrete after initial cracking or debonding.

The welded extensions with rod acted as mechanical interlock and anchored the top steel plate to the concrete. The lateral separation of sheeting from concrete in WER beams was delayed compared to OS and WE beams. With continued loading, concrete cracked at the interface of extension plate (stage 3) causing interlocking force to deteriorate that initiated the lateral separation (stage 4) of steel at the top. At the same time, slip between steel and concrete (stage 4) was observed at the ends of the beam. As the lateral separation continued, the tag welds between extension plate and main steel skin (stage 5) started to fail. This enhanced the outward separation of steel and widened the gaps between extension plate and concrete core. Before the ultimate load, interface cracks propagated to the sides and deep insight into the concrete core. At the failure stages, side steel plates buckled outward and took the cracked concrete with it. After the ultimate load, the steel skins buckled outwards diagonally (stage 6) at the loaded points, which was followed by local bearing at the supports and the loaded points (stage 7). Lateral separation of the plate started from ends of the beam and propagated towards the loaded point as shown in Figure 4.
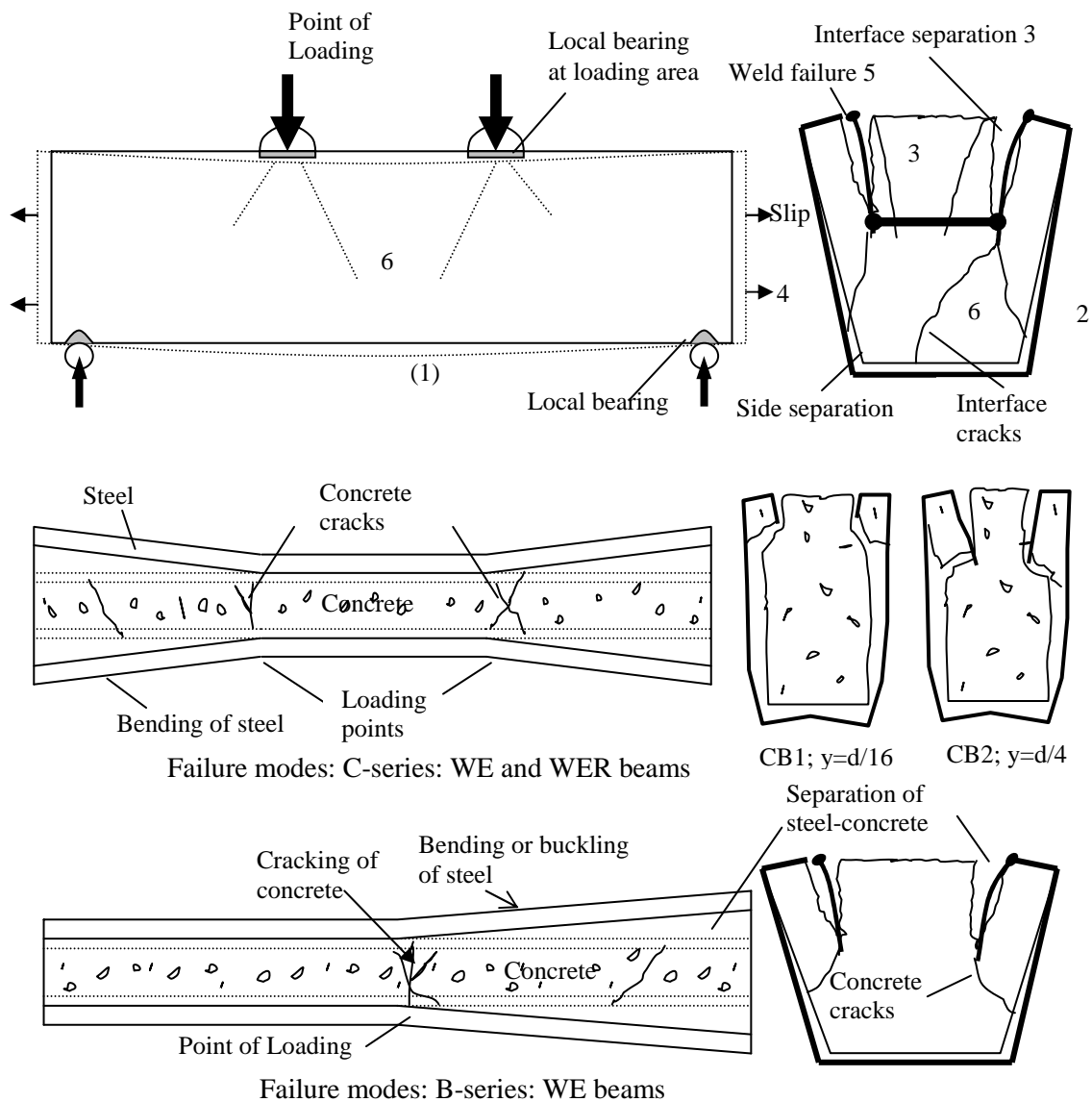
Figure 4: Failure mode 3 of TWC beams

The WE beams showed similar behaviour (mode 3) to that of WER beams although they had lower strength. Stages 5 and 7 of failure mode 3 were absent in shallow (B-series) WE beams with continuously welded extension plate. The outward buckling in such beams also propagated from one end of the beam to the centre as shown in Figure 4 while the other end showed no sign of such buckling. This might be due to the initiation of interface crack at one end and subsequent collapse of the affected end. The extension of interface cracks depends on the depth of extension (y) as can be seen from the typical failure section of beams CB1 (OS) and CB2 (WE) shown in Figure 4.
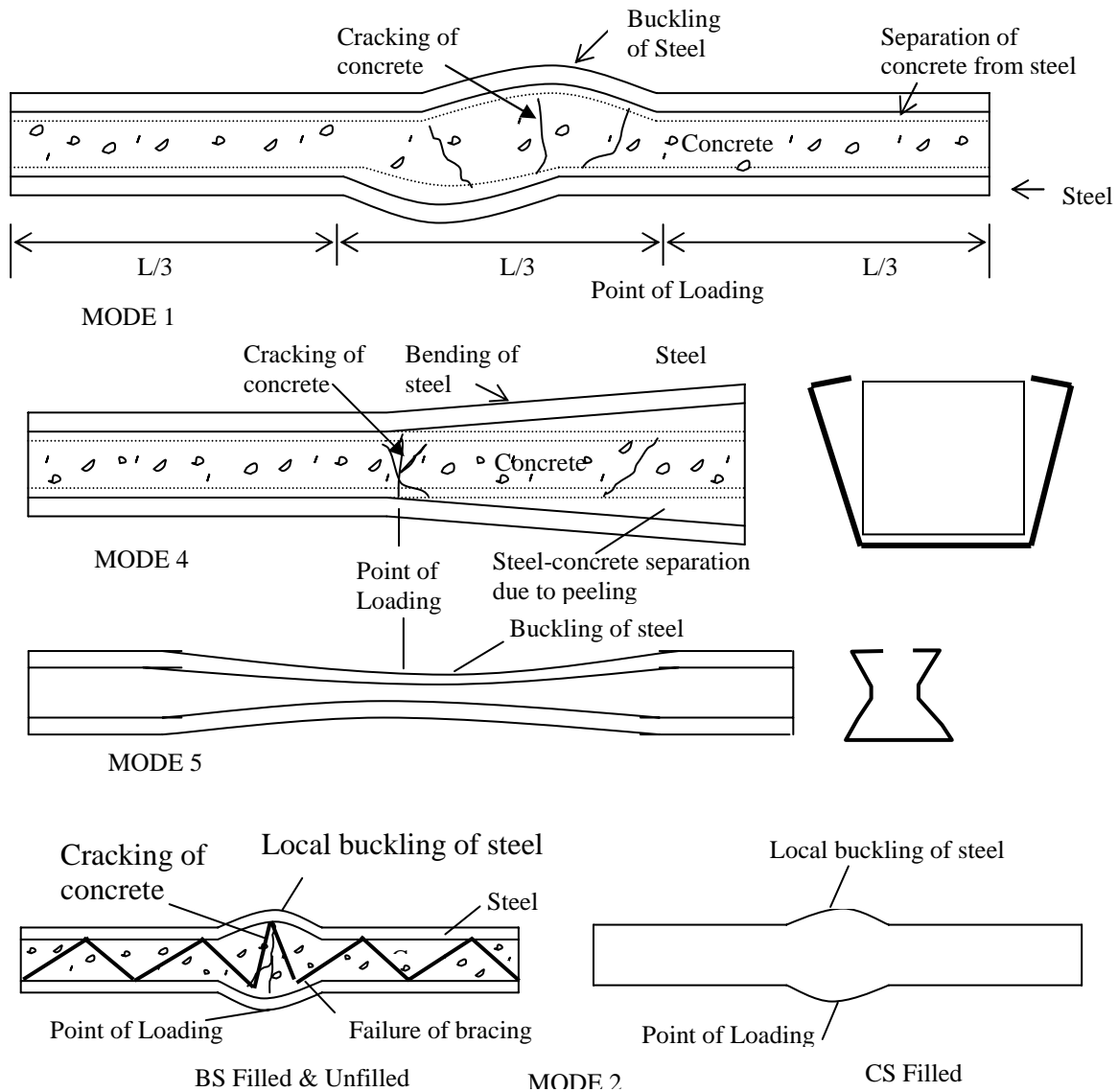
Figure 5: Failure mode 1, 2, 4 & 5 of TWC beams

After initial stages of debonding in OS beams, the lateral separation between steel and concrete started due to compression (Figure 5) in the open top flange where the steel plate is free to deform laterally. The OS filled beams failed (showing only stage 1 and 2) due to lateral separation between sheeting and concrete either concentrated at the centre (Mode 1 for slender beams) or extended to the support (Mode 4 for short beams). Unfilled OS beam (steel section only) showed different mode of failure (mode 5) than its similar filled counterpart. With progressive loading, the open side flanges were observed to buckle inwards (converging) forming a bow shape as shown in Figure 5.

BS beams exhibited better response and the separation between steel-concrete interface was negligible compared with OS beams. Typical failure mode of such beam (failure mode 2) is shown in Figure 5. The welded braces restricted the outward buckling of the top steel plates and the failure was associated with outward buckling of steel skins and concrete cracking at the point of application of load at the centre. CS beams showed failure modes (mode 2) similar to those of braced beams as shown in Figure 5. However, the strength of such beams was greater than the braced beams.

To avoid lateral separation at the top open compression flange and to enhance better interaction in OS beams, installation of connections between sheeting and concrete in the form of bracing's or extensions are essential.

3 Performance study

3.1 Performance of WE and CS beams in B3 series

Figure 6a compares the load-deflection responses of OS, WE and CS beams. The ultimate (peak) strengths of the WE beams increased with the increase of the depth of welded extension. The ductility (measured on the basis of peak deformation) of the WE beams was also higher than OS beam as could be seen from the 100% and 173% increase in the ultimate (peak) deformation.
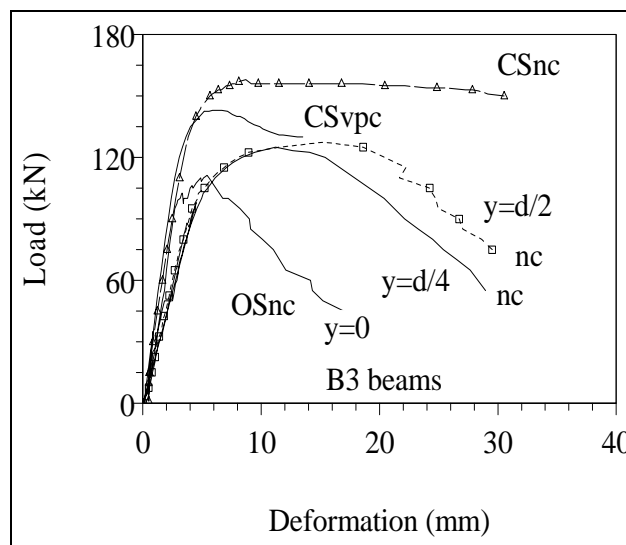

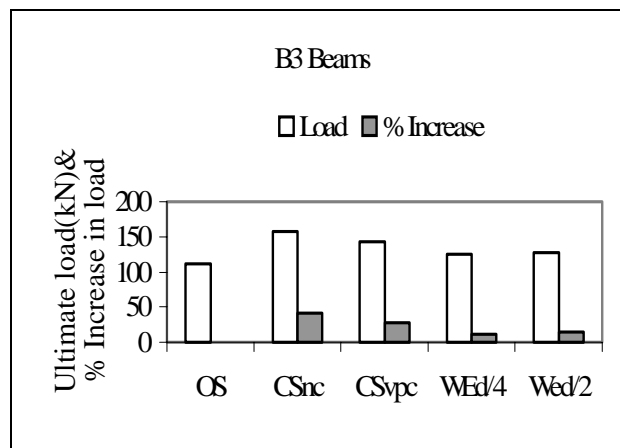**Figure 6a: Load-deflection responses**

Figure 6b: Strength enhancement

Figure 6b compares the strength of B3 beams. It is found that the strengths of CS (41% increase for NC and 28% increase for VPC) and WE (increase of 11% for y=d/4 and 14% for y=d/2) beams are higher than the respective OS beams. The ductility of CS beam was higher than OS beam (58%) but lower than WE beams (27% compared to d/4 and 73% compared to d/2).

3.2   Performance of CS and BS beams in B4 series

Figure 7a compares the load-deflection responses of such beams. From Figure 7b, it can be concluded that the strengths of CS (45% increase for NC and 38% increase for VPC) beams are higher than the respective OS beams.
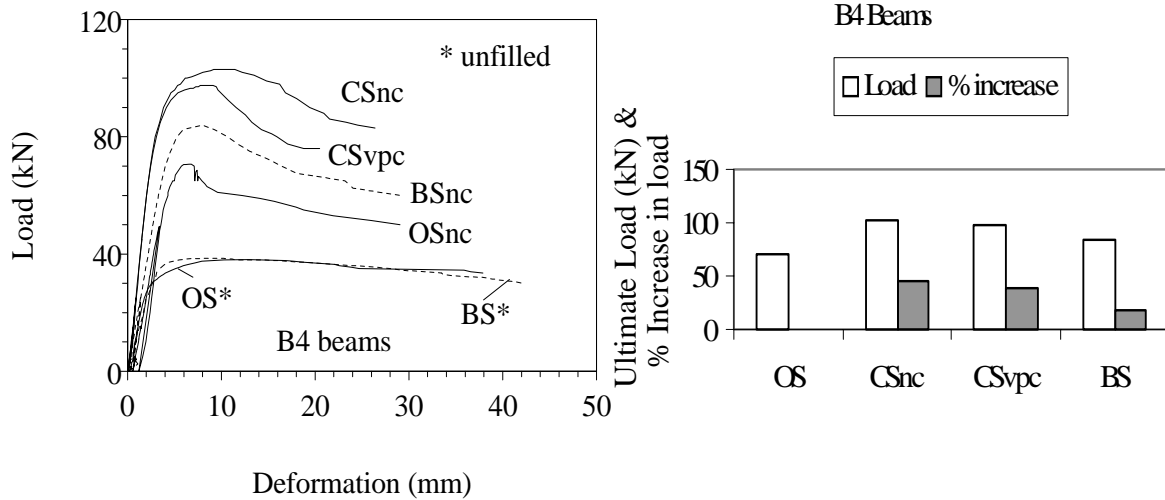

Figure 7a: Load-deflection responses   **Figure 7b: Strength enhancement**

CS beams were also ductile (70% for NC and 34% for VPC) than OS beams. The ultimate strength of BS beam was higher than OS beam (B4Inc) by 19% but less than CS beam by about 23%. The ductility of the BS beam was lower (42%) than CS beam but higher (17%) than OS beam.

3.3   Comparative Performance unfilled and filled beams

Figure 7a compares the load-deformation responses of OS and BS filled and unfilled beams. The presence of bracing in unfilled sections did not improve the strength (only 0.5% increase) and but the failure mode had been changed. The strength of the filled beams was substantially higher (46% for OS and 54% for BS) than the individual strength of unfilled steel section.
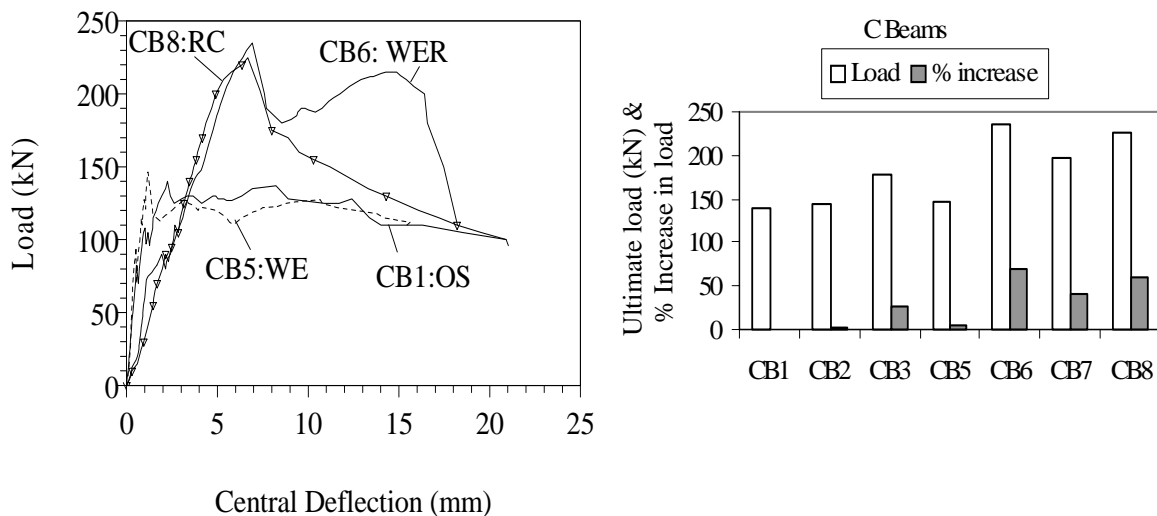

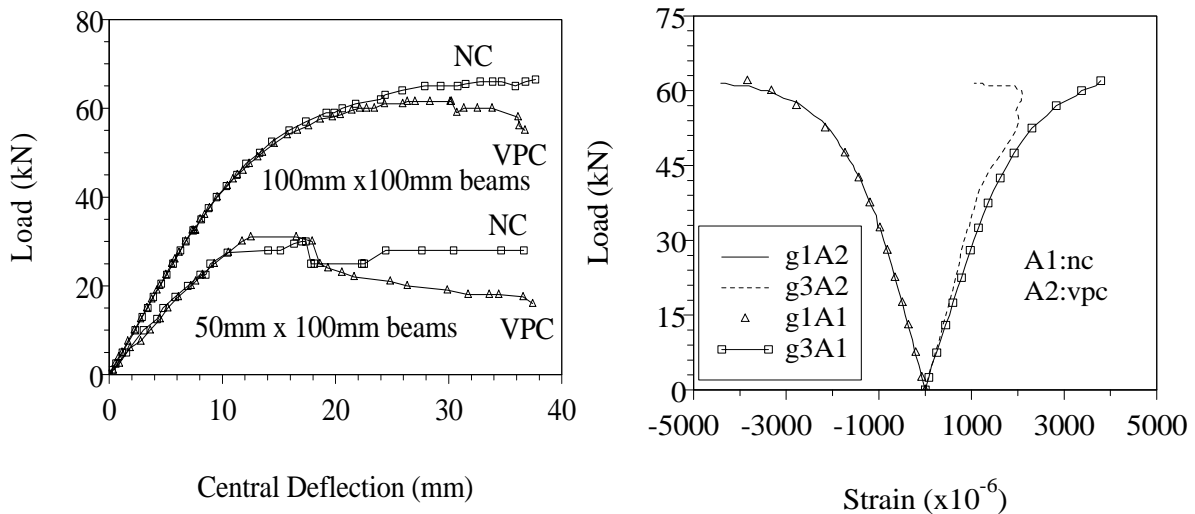**Figure 8a: Load-deflection responses**   **Figure 8b: Strength enhancement**

3.4 Performance of WE, WER and RC beams

Figure 8a-b load-deflection responses and strength development characteristics of OS, WE, WER and RC beams in C series. It was concluded that the strengths of WE (increase of 3% for y=d/4 (CB3) and 5%for y=d/2 (CB5)) and WER (increase of 26% for y=d/4 (CB3) and 69% for y=d/2 (CB6)) beams were higher than the respective OS beams. The ductility up to the ultimate load was increased by about 250% for CB2 (WE) and by about 121% for CB3 (WER) compared with CB1 (OS). It is interesting to note that although the use of welded rod enhanced the strength of CB3 (WER) by 23% but it seemed to produce lower ductility than CB2 (WE).

The enhancement of ductility seemed to be dependent on the location of the welded rod. The presence of welded rod at d/2 enhanced the ductility of CB6, while the presence of rod at d/4 reduced the ductility of CB3. This was due to the fact that the provision of welded rod at greater depth allowed more volume of concrete to be effective in the zone of influence of welded extension-rod assembly.

The strength of RC beam CB7 and CB8 was increased by 41% and 67% respectively while the ductility was also enhanced by 216% and 197% respectively.

The strength and ductility of CB6 (WER) beam were higher than any other beam in the series C. This implies that it will be possible to design TWC beams with welded rod and hook assembly without using longitudinal and shear reinforcements.

Figure 9a: Performance of NC and VPC beams   Figure 9b: Strain characteristics

3.5 Effect of VPC on TWC beams

Figures 9a and 7a compare the load deflection responses of OS (series A) and CS (B3 and B4) beams. It is revealed that both NC and VPC beams performed in similar manner when compared on the basis of strength and ductility, although the strength of NC beams are 5-10% higher than VPC beams having similar concrete strength.

The typical variation of bending strains in series A beams with VPC and NC in-fill is shown in Figure 9b. Both VPC and NC beams show similar pattern of variation. It seemed to be that the type of concrete has less influence on the strain.

3.4   Strain Characteristics

Both tensile and compressive strains in OS beams in Series A (Figure 9b) and only tensile strains in OS beams in series C exceeded yield strain at about 75% to 98% of ultimate load. This indicated that analytical models for these beams could be developed based on the yielding of the tensile steel plate. None of the strain gauges in WE and WER C-beams registered yield strain [1](Hossain, 2000). They registered only 3 to 7% of yield strain of steel. Design of such beams should therefore, be based on buckling of steel plate rather yielding of steel.

4   Design oriented Analysis

It was confirmed that the failure of the beams was affected by the presence of strength enhancement devices. The side plate debonding and buckling of steel were dependent on the cross-sectional geometry and degree of plate restraint at the edges provided by the strength enhancement device.

To develop theoretical equations, the degree of restraint achieved in beams with various modes of connection devices is to be identified to derive buckling stress of side steel plates based on experiments. A check is to be made whether the design should be based on either yielding of steel or buckling of side steel plates.

4.1   Analytical Model for flexural strength

Analytical models have been developed based on the models proposed by Oehlers et. al [9] and Hossain [10] for profiled composite beams taking into consideration of the buckling and failure modes of the experimental beams. Let us consider the TWC beam shown in Figure 10a. The design point is taken as:

The position of maximum moment at mid span at a distance L/2 from the end of the beam for single point loading. Analysis is also carried out at the position of maximum moment for two point loading both at L/3 and L/2.
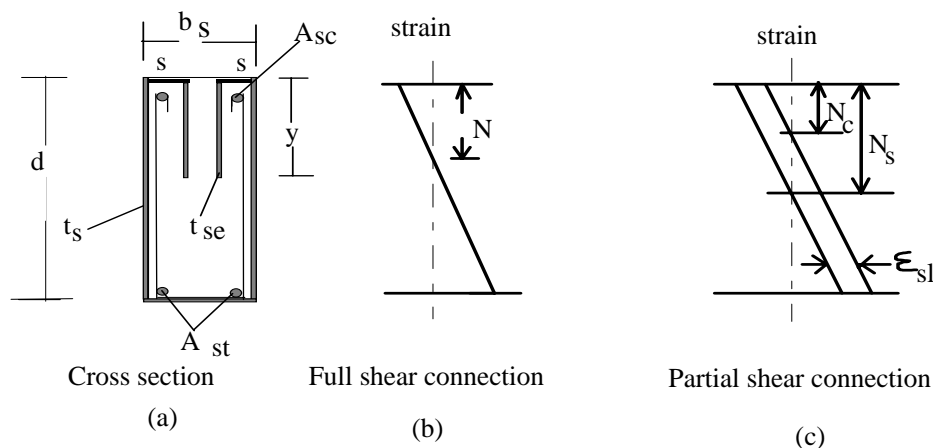

Figure 10: Strain distribution in TWC beams

Up to the limit of generated interface bond force not exceeding the interface bond strength, the composite beam will exhibit full interaction and there will be no slip across the steel-concrete interface. The same strain distribution will exist in sheeting and concrete with neutral axis of

both steel and concrete section, N, coincident to each other as shown in Figure 10b. If the maximum moment capacity is reached without the interface bond force exceeding the interface bond strength then the beam exhibits full composite action or full interaction.

But in reality, it is difficult to have full interaction in the case of composite beams. The beam exhibits partial interaction with slip occurring across the interface due to the interface bond force exceeding the interface bond strength. As a result, there will be a steep change, ε_{sl} between the strain in sheeting and concrete as shown in Figure 10c. The position of the neutral axis for concrete N_C will be different than the steel sheeting N_S. According to Oehlers [11], the slip strain is assumed to be constant throughout the depth of the beam that leads to a uniform slip at the ends.

Concrete section

Sheeting section
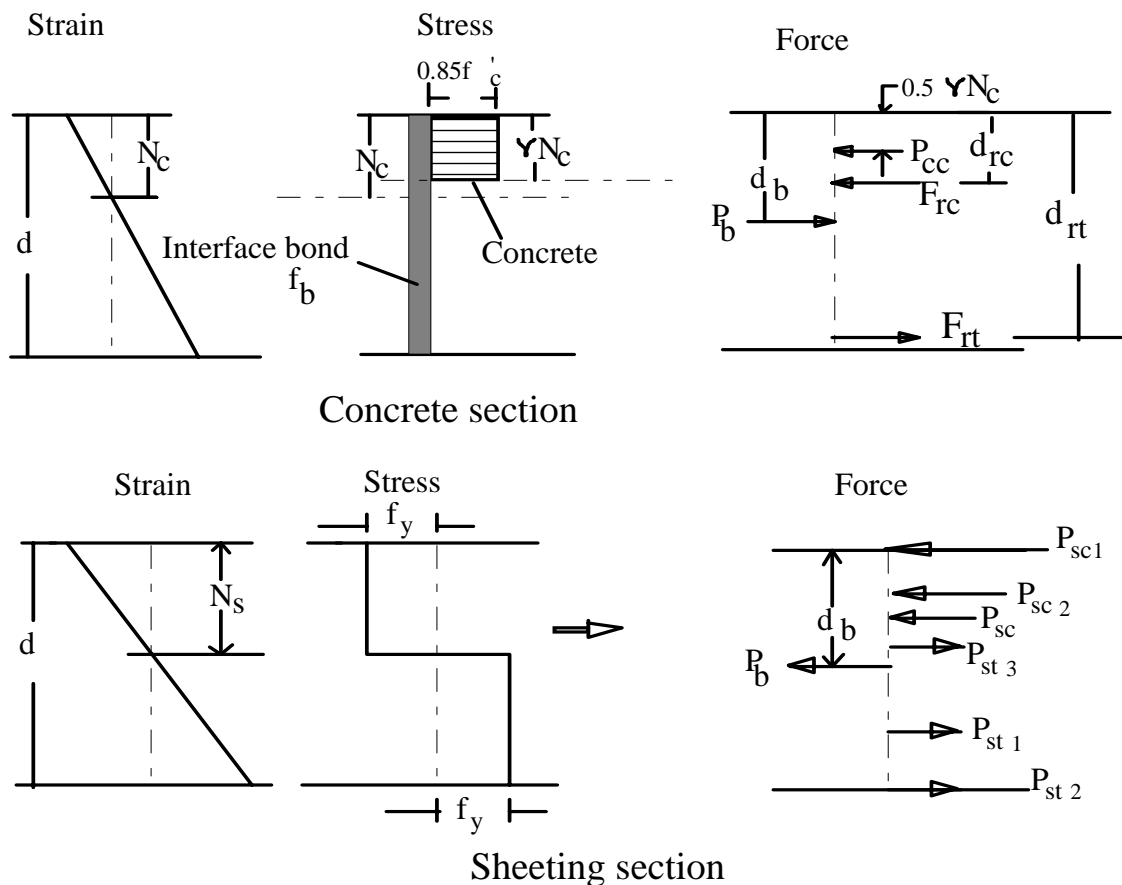
Figure 11: Distribution of forces

The flexural strength of the composite beam can be determined by considering the distribution of forces in the concrete and steel sections. The distribution of forces in the individual concrete and steel sections is shown in Figure 11.

Partial shear connection

For partial shear connection, $N_C \neq N_S$. Considering the equilibrium of forces in concrete

$$F_{rc} + P_{CC} = F_{rt} + P_b$$

$$A_{sc}f_{rc} + 0.85f_c'\gamma N_c b_c = P_b + A_{st}f_{rt} \tag{1}$$

Where F_{rc}= force due to compressive steel, P_{cc}= Compressive force due to concrete, P_b= force due to shear bond, F_{rt}=Tensile force due to bottom steel, f_{rc}= stress in the compression steel at the top and f_{rt}= stress in the bottom tensile steel. The factor γ can be related to the compressive cylinder strength (f'c) of concrete and can be calculated from the equation (AS3600,1988): γ=0.85-0.007*(f'c-28).

Considering both tension and compression rods are at yield, the equation for N_C can be derived as:

$$N_c = \frac{P_b + F_{rt} - F_{rc}}{0.85f_c'\gamma b_c} = \frac{P_b + A_{st}f_y - A_{sc}f_y}{0.85f_c'\gamma b_c} \tag{2}$$

where f_y= yield strength of the steel rods, b_c=width of net concrete section and is approximated as b_s-2t_s-2t_{se}

From strain compatibility, for both steel to be yielded, the condition is:

$$\varepsilon_{sc} = \varepsilon_u \frac{N_c - d_{rc}}{N_c} .....or..\varepsilon_{st} = \varepsilon_u \frac{d_{rt} - N_c}{N_c} \geq \varepsilon_{sy}(=0.002) \tag{3}$$

Where ε_{sc}= strain in the compression steel, ε_{st}= strain in the tensile steel, ε_u= maximum compressive strain of concrete=0.003, ε_{sy}= yield strain of steel, d_{rc}= depth of the compression steel from top and d_{rt}= depth of the tensile steel from top.
If the compression steel is not at yield, then N_c is to be recalculated based on actual stress-strain condition in the compression steel. The stress f_{rc} in the compression steel can be taken from:

$$f_{rc} = E_s\varepsilon_{sc} = E_s\varepsilon_u \frac{N_c - d_{rc}}{N_c} \tag{4}$$

Where E_s= Modulus of elasticity of steel
The value of N_c for the case when compression steel is not at yield can be derived by putting the value of f_{rc} from equation 4 to equation 1, leading to the following quadratic equation:

$$(0.85f_c'\gamma b_c)N_c^2 + (A_{sc}E_s\varepsilon_s - A_{st}f_y)N_c - P_b - A_{sc}d_{rc}E_s\varepsilon_u = 0 \tag{5}$$

The interface bond force of the beam can be written as: $P_b= \sum_o \times f_b$
where $\sum_o$ = cross-sectional perimeter of steel sheeting in contact with concrete, x = L/2 or L/3 and f_b = shear bond stress at the interface.

The maximum shear bond stress [12] (Patrick,1990) at the sheet-concrete interface due to mechanical interlock in the form of different types of embossment rolled into the sheet ranges from 0.2 to 0.5 N/mm². For plain profile sheeting with no embossments, a value of 0.1N/mm² can be used.

Considering the case of welded extension extending below the neutral axis (y>N_s) and from the equilibrium of steel section (Figure 11):

$$P_b + P_{sc} + P_{sc1} + P_{sc2} = P_{st1} + P_{st2} + P_{st3}$$

$$P_b + 2f_{sy}N_s t_s + 2f_{sy}N_s t_{se} + 2f_{sy}t_s s = 2(d - N_s)f_{sy}t_s + b_s t_s f_{sy} + 2(y - N_s)t_{se}f_{sy} \quad (6)$$

where P_b= Bond force, P_{sc}, P_{sc1} and P_{sc2} are the compressive forces in the web, top and welded extension steel above the neutral axis respectively; P_{st1}, p_{st2} and p_{st3} are the tensile force in the web, bottom and welded extension steel below the neutral axis respectively and f_{sy}= yield stress of steel plate.

$$N_s = \frac{f_{sy}t_s(2d + b_s - 2s) + 2yt_{se}f_{sy} - P_b}{4(t_s f_{sy} + t_{se}f_{sy})} \quad (7)$$

The depth of the neutral axis N_s considering the yielding of steel can be derived as:

For the case of no welded extension (y=0), N_s can be derived as:

$$N_s = \frac{f_{sy}t_s(2d + b_s - 2s) - P_b}{4(t_s f_{sy})} \quad (8)$$

Taking moment of all the forces about the top fibre of the beam, the moment capacity (M_u) of the TWC beam with doubly reinforced concrete core considering partial interaction can be determined from the expression:

$$M_u = t_s f_{sy}(d^2 + db_s - 2N_s^2) + t_{se}f_{sy}(y^2 - 2N_s^2) + f_{rt}A_{st}d_{rt} - f_{rc}A_{src}.d_{rc} - 0.425\gamma^2 N_c^2 b_c f_c' \quad (9)$$

For plain concrete core with welded extension (y>N_s), the equation reduces to:

For plain concrete without welded extension (y=0), the equations become:

$$M_u = t_s f_{sy}(d^2 + db_s - 2N_s^2) + t_{se}f_{sy}(y^2 - 2N_s^2) - 0.425\gamma^2 N_c^2 b_c f_c' \quad (10)$$

$$M_u = t_s f_{sy}(d^2 + db_s - 2N_s^2) - 0.425\gamma^2 N_c^2 b_c f_c' \quad (11)$$

For plain concrete with welded extension not extending below the neutral axis (y<Ns), the equation becomes:

$$M_u = t_s f_{sy}(d^2 + db_s - 2N_s^2) - t_{se}f_{sy}(y^2) - 0.425\gamma^2 N_c^2 b_c f_c' \quad (12)$$

For doubly reinforced with welded extension not extending below the neutral axis (y<Ns), the equation becomes:

$$M_u = t_s f_{sy}(d^2 + db_s - 2N_s^2) - t_{se}f_{sy}(y^2) + f_{rt}A_{st}d_{rt} - f_{rc}A_{sc}.d_{rc} - 0.425\gamma^2 N_c^2 b_c f_c' \quad (13)$$

Full connection

For full shear connection, N_C=N_S, thus equating equations 2 and 7, the bond strength P_{bfc} required to achieve full shear connection, can be determined as:

$$P_{bfc} = \frac{0.85f_c'\gamma b_c[f_{sy}t_s(2d + b_s - 2s) + 2yt_{se}f_{sy}] - (A_{st}f_{rt} - A_{sc}f_{rc})(4t_s f_{sy} + 4t_{se}f_{sy})}{0.85f_c'\gamma b_c + 4t_s f_{sy} + 4t_{se}f_{sy}} \quad (14)$$

Substituting the value of P_b from equation 14 in equations 2 and 7 will allow the determination of N_c and N_S. The moment capacity for full shear connection can be obtained by substituting the value of N_c and N_S in equation 9.

To cause both compression and tension steel rods to yield simultaneously, more bond strength is necessary for full composite action.

## 4.2   Application of the analytical models in design

The performance of the analytical model is validated through test results of experimental beams. The proposed design equations 2, 7, 9 and 14 are used to simulate the behaviour of experimental beams by using the following:

- Geometric parameters: for series A beams: y=0, A_{rc}=0, A_{rt}=0; for series B beams: y=variable, A_{rc}=0 and A_{rt}=0 ; for series C beams: y=variable , A_{rc} and A_{rt} are included in reinforced beams. The effect of welded rods at the end of the extension plates is not taken into account.
- Considering buckling stress of steel plate is higher than the yield strength which means that the buckling commences after yielding.
- Appropriate check has been made whether both top and bottom steel or only bottom steel is yielded in the doubly reinforced beam analysis of TWC reinforced beams (CB7 and CB8).

4.2.1 Effect of interface shear bond (p_b)

The performance study of all the beams using analytical model has been performed by varying the shear bond stress (p_b) that simulates the degree of interaction between sheeting and concrete. The degree of interaction between sheeting and concrete in actual experiments varies due to the presence of welded extension, bracing's and welded rods. By varying p_b, it is possible to simulate the degree of interaction and the performance of various mechanical devices used in the experiments to enhance the interface bond.

The typical effect of p_b on strength and the values of N_c and N_s is presented in Figures 12 for C beams. Similar patterns of variation are observed for beams in all series. The ultimate strength of all the beams increases with the increase of p_b from 0.2N/mm^2 to an optimum value, P_{bopt}, (full shear bond capacity, P_{bfc}) and then started to decrease. The value N_c increases with the increase of p_b and the value of N_s decreases with the increase of P_b. The bond stress at the intersection point between N_c and N_s and p_{bopt} represent the shear bond for full composite action. Both values exactly correspond to the full shear bond calculated based on equation 14. P_{bfc} values for the beams are presented in Table 2.
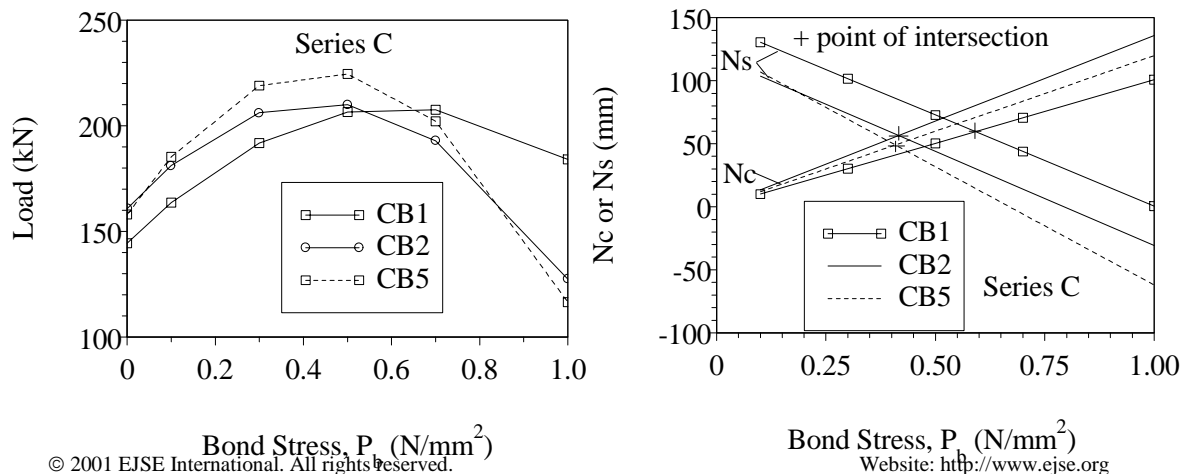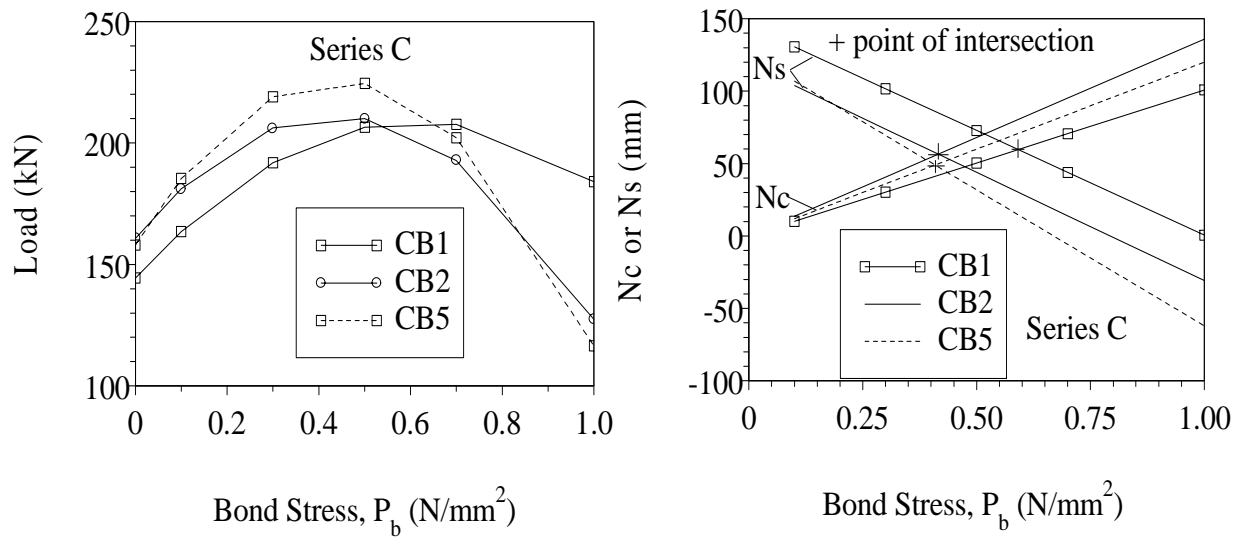
Figure 12: Typical variation of N_c or N_s and ultimate load with P_b for C beams

The p_{bfc} values (Table 2) for OS beams vary from 0.25 to 0.4 MPa in series A and 0.6 to 0.7 in series B and C. For WE beams it varies from 0.36 to 0.42MPa (series B and C), for CS beams (series B) vary from 0.33 to 0.47 MPa and for BS beams (series B) about 0.44 MPa.

The p_{bfc} for OS beams is higher than CS, BS and WE beams. This means that degree of interaction in WE beams are higher than the other beams. Similar phenomena are observed in series C with OS beams with or without reinforcing steel need more P_{bfc} than beams with welded extension. The contribution of welded rods is not reflected in the values, as it is not included in the design formulations.

The interface shear bond required to have full shear connection could be attained by using mechanical devices as used in the experiments. Analytical calculations are performed with interface shear bond of 0.1 N/mm^2 for partial shear connection which is typical for plain sheeting [12].

Table 2: Comparison of experimental and theoretical analysis

Beam	Proposed Analytical Models Ultimate load and Moment			Expt.	Ratio	
	Full Connection		Partial Connection		Full	Partial
	P_{fc} (M_{fc})	Full bond p_{bfc}	$p_b=0.1N/mm^2$ P_{pc} (M_{pc})	$P_{exp}(M_{exp})$	P_{exp}/P_{fc}	P_{exp}/P_{pc}
	kN(kNm)	N/mm^2	kN (kNm)	kN (kNm)	M_{exp}/M_{fc}	M_{exp}/M_{pc}
A1:nc	65.4(16.4)	0.44	59.39(14.9)	66.5(16.6)	1.02	1.12
A2:vpc	65(16.3)	0.42	59.37(14.9)	65(16.3)	1.00	1.09
A3:nc	30.8(7.7)	0.25	29.55(7.4)	30.8(7.7)	1.00	1.04
A4:vpc	30.7(7.6)	0.24	29.53(7.4)	31.5(7.9)	1.03	1.07

B3Inc	110(16.4)	0.73	97(14.5)	111(16.7)	1.02	1.15
B3IInc	130(19.5)	0.48	124(18.5)	158(23.7)	1.21	1.28
B3IIvpc	130(19.5)	0.46	124(18.5)	143(21.5)	1.10	1.16
B3d/4nc	124(18.5)	0.38	120(18)	125(18.8)	1.01	1.04
B3d/2nc	124(18.5)	0.36	119(17.9)	128(19.1)	1.03	1.07
B4Inc	55(8.2)	0.56	48(7.2)	71(10.6)	1.29	1.47
B4IInc	59(8.8)	0.33	56(8.4)	103(15.5)	1.75	1.83
B4IIvpc	59(8.8)	0.33	56(8.4)	98(14.6)	1.66	1.73
B4IIInc	61(9.1)	0.44	56(8.4)	84(12.6)	1.39	1.49
CB1	208(34.3)	0.59	164(27.0)	140(23.1)	0.67	0.86
CB2	208(34.4)	0.42	182(28.0)	144(23.8)	0.69	0.79
CB3	208(34.4)	0.42	182(28.0)	170(28.10	0.82	0.94
CB4	222(36.6)	0.49	181(29.9)	177(29.2)	0.80	0.98
CB5	222(36.6)	0.42	185(30.6)	147(24.2)	0.66	0.79
CB6	223(36.8)	0.42	185(30.6)	235(38.8)	1.05	1.27
CB7	293(48.4)	0.70	205(33.8)	198(32.7)	0.67	0.96
CB8	293(48.4)	0.70	205(33.8)	225(37.8)	0.77	1.10
Values in the brackets are moments in kNm; E_s= 210000MPa						

5.0   VALIDATION OF THEORETICAL MODELS & RECOMMENDATION

The moment capacities and the resulting ultimate loads for both full and partial shear connections are compared with those from experiments in Table 2. Both partial and full shear connection analyses (based on yielding of steel) predict the moment and load capacities of series A and B beams satisfactorily. Analytical models with both full and partial connections (Table 2) under-predict the ultimate capacities but seem to be safe with experimental to theoretical ratio ranges from 1.0 to 1.75 (full connection) and from 1.04 to 1.83 (partial shear connection). Factor of safety is higher for braced or fully closed beams (1.49 to 1.83) but these beams may not be practically feasible.

Both series A and B beams can be safely designed based on either full or partial shear connection analysis. However, partial shear connection analysis has better factor of safety and therefore, recommended for design purposes.

Full or partial shear connection analysis seems to over estimate the ultimate moment and load capacities of most of the series C beams except WER (CB6) and RC beams with main and shear reinforcement. The ratio of experiment to theory ranges from 0.67 to 0.82 for full connection and from 0.79 to 0.98 for partial shear connection analysis. Therefore, using prediction based on

yielding of steel does not provide any factor of safety in the design. The overprediction may be due to the following reasons:

1. Buckling of steel occurred before yielding in these beams. It was confirmed from the experimental strain readings of C-beams that the strains were well below the yield strain at ultimate load compared with A beams where yield strain was observed before the beam reached ultimate load. Hence, the use of yield stress in the analytical models will overpredict the strength of the C beams.

2. The steel skins used in A and B beams were commercial square and rectangular hollow sections and are much stiffer than that used in C-beams made in the house. The d/t_s (slenderness) ratios of C beams are 4 to 5 times higher than those of A and B beams (Table 3). Consequently buckling stress of steel plates in series C beams should be much lower than series A and B beams. As a result the side steel plates will buckle before the yielding of steel.

To apply theoretical equations, the buckling stress of steel plates should be checked with appropriate boundary conditions. The solution to the buckling of flat isotropic plates simply supported on all four sides subjected to uniaxial uniform compressive in-plane loads has been treated in the past. However, for many other boundary conditions, simple displacement functions do not exist, and in some cases analytical, exact solutions have not been found. In such cases approximate solutions have been found using energy methods.

Parametric studies have been conducted on side steel plates with boundary condition closely representing the beams considering two loaded sides hinged and other two sides with variable restraint subjected to in-plane bending loads (Figure 13). For rectangular plates subjected to in-plane bending loads, the equation 15 can be [1] used to determine the buckling stress (σ_b) of the plate:

$$\sigma_b = \frac{k_b \pi^2 E_s}{12(1-v^2)} \left(\frac{t_s}{d}\right)^2 \tag{15}$$

The bending buckling co-efficient k_b can be taken from Figure 13 for different degree of rotational restraint (ε) to calculate the buckling stress. For practical cases of TWC beams aspect ratio, L/d, of the plate should not be less than 7 except for deep beams. It can be seen from the graphs (Figure 13) that the value of k_b is not sensitive to the variation of aspect ratio greater than 7.
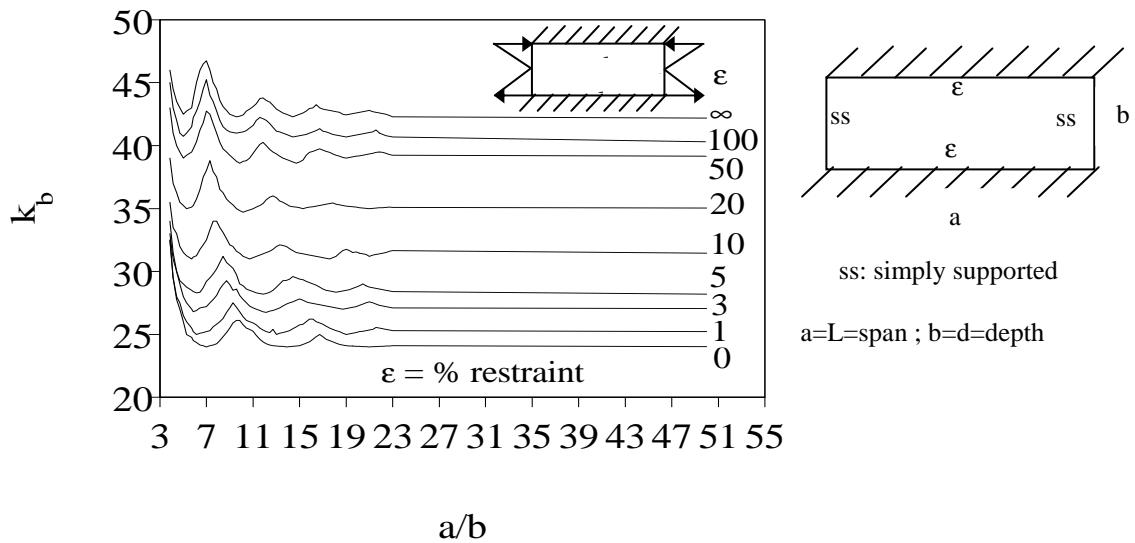
a/b

Figure 13: Design chart for the determination of buckling co-efficient (k_b)

The degree of rotational restraint (ε) at the top and bottom of the side plates can be varied from 0% to infinity. The 0% represents simply supported edges while infinity represents fully clamped. Practical values depend on the degree of restraint achieved in various TWC beams with various modes of connection devices. Parametric studies have been performed to relate degree of restraint (ε) to the various modes of connection devices. The buckling stresses was calculated with various degree of restraint (ε) and then used in the analytical equations to calculate the ultimate capacity of the beams. The degree of restraint for each beam is identified based on good agreement between experimental and theoretical capacities.

Buckling stresses of side steel plates for beams in series A, B and C are calculated using equation 15 and Figure 13 for different degree of restraint and presented in Table 3. It is found that the beams in series A and B (having lower d/t_s ratio compared with C beams) have buckling stress much higher than the yield stress even at 0% restraint. This means that in these beams, yielding of steel commences before buckling and the design based on yielding of steel governs. Good agreement (Table 2) between theoretical and experimental capacities for A and B beams confirms the fact. The minimum d/t_s ratios needed to initiate buckling is much higher than the actual d/t_s ratios present in series A and B beams (as can be seen from Table 3) that ensure yielding before buckling.

Table 3: Analysis of buckling stress for different degree of restraint

		Buckling stress (σ_b) in MPa : based on equation 15	Based on Eq. 15
Beam	d/ts	Degree of restraint (ε) 0% 5% 10% 20% 30% 40% 50% 100% Infinity	Minimum d/t_s required for yielding
A1, A2	31.25	4553	109 Yield
A3, A4	43.48	2352 exceeded yield stress (275 or 250MPa) at 0% restraint	112.71 Yield
B3	31.25	4553	109 Yield

B4	43.48	2352 exceeded yield stress (275 or 250MPa) at 0% restraint									112.71 Yield
C	156.25	182	213	243	273	288	296	303	319	333	131.54
		up to 20% restraint exceeds yield stress of 257MPa									Buckling
C	**156.25**	**Values of k$_b$ for different degree of restraint**									
		24	**28**	**32**	**36**	**37**	**38**	**40**	**42**	**44**	

The buckling stress and k$_b$ values for different degree of restraint for C-beams are also presented in Table 3. Actual d/t$_s$ ratios in these beams is much higher than that needed for buckling which ensure commencement of buckling before yielding. The use of yield stress for the determination of strength of such beams as presented in Table 2, therefore, overpredicted the strength.

Table 4: Strength prediction of C-beams incorporating buckling stress

Beam	% restraint (ε)	k$_b$	σ$_b$ MPa	P$_{buc}$ (M$_{buc}$) kN (kNm)	P$_{exp}$ (M$_{exp}$)	P$_{exp}$/P$_{pc}$ M$_{exp}$/M$_{pc}$
CB1	**0**	24	182	133.7(22.06)	140(23.1)	1.05
OS	5	28	212.5	154(25.4)		
CB2	**0**	24	182	133.6(22.05)	144(23.8)	1.08
WE	5	28	212.5	153(25.3)		
CB3	0	24	182	133.6(22.05)	170(28.1)	
WER	5	28	212.5	153(25.3)		1.11
	10	32	243	172.3(28.4)		0.99
	20	36	273	192(31.6)		
CB5	**0**	24	182	138.5(22.8)	147(24.2)	1.06
WE	5	28	212.5	157.5(26)		
CB6	0	24	182	138.5(22.8)	235(38.8)	
WER	5	28	212.5	157.5(26)		
	10	32	243	176.6(29.1)		
	20	36	273	195(32.2)		
	30	38	288	204.6(33.8)		1.15
CB7	0	24	182	143(23.6)	198(32.7)	
CB8	5	28	212.5	160.6(26.5)		
	10	32	243	178(29.3)		
	20	36	273	195(32.3)		1.02

Bold figures represent degree of restraint needed to reasonably simulate experimental values

But for series C beams, using different degree of restraint, it is possible to have a good agreement between theoretical and experimental capacities. The analytical ultimate loads and moments calculated based on buckling stress with different degree of restraint using partial shear connection are presented in Table 4. It can be seen from Table 4 that OS and WE beams can be designed with 0% restraint.

On the other hand for WER beams, 30% restraint should be used in design. It is recommended that for open beams, 0% restraint and for beams with welded extension and rod, 20% restraint will provide a safe design. The ratio of experimental to predicted values (derived from appropriate degree of restraint) ranges from 1.02 to 1.15 that shows reasonable agreement. Hence, theoretical models incorporating buckling stress with appropriate degree of restraint and partial shear connection can safely be used for design.

5   Conclusions

Comprehensive series of tests revealed the performance of various modes of interface connections on the strength enhancement of beams. The strength of the beams is limited by the compression buckling capacity of the steel plate at the top of the open box section. The enhancement of the strength can be possible by stiffening the compression steel plates at the open end of box section with various modes interface connections.

The strength and ductility of WER beams are higher than OS, CS, BS and WE suggesting feasibility of the design of such TWC beams in practical circumstances. The performance of CS beams was better than OS, BS, WE beams while the strength of BS beams is also higher than OS beams. TWC beams with VPC exhibited satisfactory performance compared with normal concrete that validated the viability of the use of VPC in such construction.

Analytical models have been developed for the flexural design of TWC beams using both full and partial shear connection. To apply theoretical equations, buckling stress of side steel plates should be checked with appropriate boundary conditions. The degree of rotational restraint (ε) at the top and bottom of the side plates can be varied with 0% representing simply supported edges and infinity representing fully clamped. The degree of restraint achieved in beams with various modes of connection devices is identified based on good agreement between experimental and theoretical capacities. Proposed design charts for the determination of buckling co-efficient (k_b) can be used to calculate the buckling stress of side plates with different degree of edge restraint.

The following guidelines are proposed in using analytical models for the safe design TWC beams:

- Designer's can choose the geometry (especially d/t_s ratio) of the steel section so that the design can be based on either yielding of steel or buckling of side steel plates. Designer's has to decide based on the structural requirement of the TWC beams.

- Use of partial shear connection

- For beams with yielding commencing before buckling, strength can be predicted by using yield stress in design equations.

- For beams with buckling commencing before yielding, strength can be predicted by using buckling stress in the design equations ensuring appropriate degree of restraint suitable for different mode of connections. For practical design purposes, 0% restraint (for open and welded extension beams) and up to 20% restraint (for beams with welded extension and rod assembly) are suggested.

- Proposed design equations can also be used for the design of VPC TWC beams.

6 Acknowledgment

7 References

1   Hossain, K.M.A , Behaviour of thin walled composite sections as structural elements, Proce. of the Australasian Structural Engineering Conference, Auckland, 30 Sept.-2 October, vol. 1, pp. 175-180, 1998 (ISBN 0-473-05481-7).

2   Hossain, KMA , Performance of Volcanic pumice concrete with especial reference to high-rise composite construction, Innovation in Concrete Structures: design and construction, Edited by R.K. Dhir and M. R. Jones, Thomas Telford Publishing, London, UK, pp. 365-374, September, 1999 (ISBN 0 7277 28245).

3   Hossain KMA and Mol L , Thin walled composite construction using volcanic pumice concrete, Proce. of the IEPNG International Conference, September 25-27, Rabaul, PNG, pp. 17-24, 1998.

4   Hossain K.M.A, Mol, L. and Wright H.D, Behaviour of thin walled composite beams and columns, Proce. of 2nd International Conference on Thin-walled Structures, Singapore, 2-4 December, 1998.

5   Hossain KMA , Behaviour of thin walled composite beams, Research Report No. CE-SE00-1, Department of Civil Engineering, The PNG University of Technology, Lae, Papua New Guinea, 2000.

6   Mol, LTK, Behaviour of thin walled composite structural elements, MPhil Thesis, Department of Civil Engineering, University of Technology, PMB, Lae, Papua New Guinea, 2001.

7   Hossain KMA, Development of Mix-design charts for Volcanic ash and pumice concrete, Research Report No. CE-SE97-5, Department of Civil Engineering, PNG University of Technology, Lae, Papua New Guinea, 1997.

8   Hossain KMA, Properties of volcanic ash and pumice concrete, IABSE Colloquium: Concrete Model Code for Asia, Phuket, Thailand, IABSE Report, Vol. 80, 1999, pp. 145-150, 1999. (ISBN 974-331-139-4).

9   Oehlers, D. J, Wright, H. D. and Burnet, M. J., Flexural Strength of Profiled Beams, Journal of Structural Engineering, Vol. 120, No. 2, pages 378-393,1994.

10 Hossain, K.M.A., In-Plane Shear Behaviour of Composite Walling with Profiled Sheeting, PhD. Thesis, University of Strathclyde, Glasgow, United Kingdom, 1995.

11 Oehlers, D. J., Composite Profiled Beams, Journal of Structural Engineering, Vol. 119, No. 4, pages 1085-1100, 1992

12 Patrick, M., A new partial shear connection strength model for composite slabs, Journal of Australian Inst. Steel Res. 24(3) 2-17, 1990.

Notations

b_s, d, L	:	width, depth and span of the beams respectively
o, s,y	:	width of opening, top stripped steel and length of WE respectively
MR, NMR, NS	:	main reinforcement, no main reinforcement, no stirrup respectively
t_s , t_{se}	:	thickness of steel and welded extension plate respectively
A_{st}, A_{sc}	:	area of bottom and top steel rods respectively
ν, E_s	:	Poisson's ratio and Modulus of elasticity of steel respectively
P_{fc}, M_{fc}	:	Ultimate load and moment for full shear connection respectively;
P_{pc} , M_p	:	Ultimate load and moment for partial shear connection respectively
P_{exp} , M_{exp}	:	Experimental load and moment respectively